

Electron-hybridon interaction in a quantum well

B. K. Ridley

Department of Physics, University of Essex, Wivenhoe Park, Colchester, Essex CO4 3SQ, England

(Received 16 December 1991; revised manuscript received 15 June 1992)

The confinement of optical modes of vibration in a quantum well of polar material is described by a theory involving the triple hybridization of LO, TO, and IP (interface polariton) modes, all of which share a common frequency and in-plane wave vector. The resulting hybrids satisfy both mechanical and electromagnetic boundary conditions. The case of a quantum well with infinitely rigid barriers is shown to be one in which there are no interface modes allowed (including IP modes). The resulting guided-mode patterns resemble those obtained from microscopic theory of the AlAs/GaAs system. The hybrids are shown to exhibit strong IP-induced dispersion as a function of in-plane wave vector. Each hybrid has a scalar potential and a vector potential, neither of which is continuous at the interface. Continuity, in this respect, is limited to the energy of coherent interaction with an electron. Quantization leads to a new quantum—the hybridon. The electron-hybridon interaction is described for intrasubband and intersubband scattering in an infinitely deep quantum well. Intrasubband scattering rates are close to those derived using the Huang-Zhu model for the LO₂ guided mode. The contribution from IP modes is contained within the hybrids. It is emphasized that pure IP modes do not exist in GaAs. As a result of the lack of interface modes the intrasubband rate approaches zero as the well narrows. The intersubband rate is also calculated.

I. INTRODUCTION

The confinement of optical modes of vibration in semiconductor quantum wells and its effect on the Fröhlich interaction with electrons has been the subject of some interest and not a little controversy¹ in recent years. The first model of confinement, dating back to the investigations of Fuchs and Kliewer² into the vibrations of thin ionic slabs, described confinement in terms of satisfying electromagnetic boundary conditions and treating the medium as an isotropic dielectric continuum (DC). This DC model failed to satisfy mechanical boundary conditions, nor did it take into account the dispersion of LO and TO modes. A second continuum model was proposed by Babiker,³ in which confinement of LO modes was described in terms of hydrodynamic boundary conditions and dispersion was taken into account, but it implicitly agreed with the DC model as regards interface polaritons (IP). It was clear that the DC model could not be correct for LO modes with zero in-plane wave vectors and hence zero tangential electric fields, but it was equally clear that the HD model violated electromagnetism when the in-plane wave vector was nonzero. Numerical studies of lattice dynamics⁴⁻¹⁰ showed that the vibrational patterns did not conform to the simple predictions of either model, but Huang and Zhu (HZ) showed that guided modes could be represented by relatively simple analytic expressions which retained the odd and even parities of the simple models, while IP modes continued to be described in the usual way.⁶ The HZ model represented a significant advance, but it was not a continuum theory and nor did it describe IP components properly, and this has led several authors recently to overestimate the strength of interaction with electrons.¹¹⁻¹³

A self-consistent continuum theory for optical modes

in nonpolar material has recently become available in which it is shown that mechanical boundary conditions can be satisfied by the double hybridization of LO and TO modes both of which share the same frequency and in-plane wave vector.¹⁴ In this picture a confined mode is seen as a hybrid consisting of a linear combination of plane waves with each component retaining its longitudinal or transverse nature and its bulklike electric properties. Dispersion is fully taken into account and ensures that the linear combination is unique. Here the extension of this theory to polar material is described in some detail and simple results are given for the scattering rates for intrasubband and intersubband processes in a single quantum well, in which the barriers are taken to be infinitely rigid and the potential barriers infinitely high, roughly corresponding to the AlAs/GaAs system for Γ -valley electrons. The principal results are as follows.

(i) All vibrational patterns in GaAs are of the guided-mode type. There are no interface modes, including no IP modes. As a result, scattering rates diminish with decreasing well width.

(ii) The involvement of an IP component in each hybrid induces strong dispersion as a function of the in-plane wave vector. It also enhances intrasubband rates and intersubband rates.

(iii) Hybrids with small in-plane wave vectors are HD-like; those with large in-plane wave vectors are DC-like.

(iv) Scalar and vector potentials are not continuous across the interface, but the energy of interaction with an electron traveling coherently with the wave is continuous.

A description of the hybridization model applied to the case of rigid interfaces is given in Sec. II. Analytic expressions are given for the relative ionic displacements of “odd” and “even” hybrids and for the associated fields

and scalar and vector potentials. An informal quantization scheme is given that leads to quanta which we call hybridons. The continuity (or, rather, discontinuity) of potentials and the form of the electron-hybridon interaction are described. Section III discusses dispersion, and it is shown that certain hybrids mimic the conventional IP dispersion over a limited range of in-plane wave vectors, and there is a general trend with increasing in-plane wave vectors from HD-like parity to DC-like parity. In Sec. IV intrasubband and intersubband scattering rates are derived ignoring all contributions from barrier modes in the spirit of the rigid-boundary approximation. Section V contains a brief discussion.

II. HYBRID MODES

One of the simplest conceptual systems is a single quantum well with infinitely rigid barriers. The boundary conditions to be satisfied are (a) the vanishing of all ionic displacement \mathbf{u} ; (b) the continuity of the tangential component of electric field, E_x ; and (c) the continuity of the normal component of electric displacement, ϵE_z , where $\epsilon(\omega)$ is the permittivity. TO modes with polarization normal to the plane of incidence satisfy these conditions without hybridizing, but they do not interact with electrons in our model and so can be ignored. Assuming elastic isotropy, we take the x axis to be parallel to the direction of propagation in the plane, and consider the three types of mode with ionic displacements with x and z components, where the z axis is perpendicular to the plane.

A. LO mode

$$\begin{aligned} u_x &= k_x (A e^{ik_L z} + B e^{-ik_L z}) e^{i(k_x x - \omega t)}, \\ u_z &= k_L (A e^{ik_L z} - B e^{-ik_L z}) e^{i(k_x x - \omega t)}. \end{aligned} \quad (1)$$

These components satisfy the LO condition $\nabla \times \mathbf{u} = 0$. The electric fields associated with these displacements are well known and given by

$$\begin{aligned} E_x &= -\rho_0 u_x, \quad E_z = -\rho_0 u_z, \quad \rho_0 = \frac{e^*}{\epsilon_0 V_0}, \\ e^{*2} &= M V_0 \omega_{LO}^2 \epsilon_0^2 \left[\frac{1}{\epsilon_\infty} - \frac{1}{\epsilon_s} \right], \end{aligned} \quad (2)$$

where e^* is the effective ionic charge, M is the reduced mass, ϵ_0 is the permittivity of free space, $\epsilon_\infty, \epsilon_s$ are the high-frequency and static permittivities, and V_0 is the volume of the primitive unit cell. These fields are associated in turn with a scalar potential:

$$\phi = -i\rho_0 (A e^{ik_L z} + B e^{-ik_L z}) e^{i(k_x x - \omega t)}. \quad (3)$$

In an approximation which assumes that the waves have long wavelength and that the medium is elastically isotropic, the dispersion relationship can be taken to be

$$\omega^2 = \omega_{LO}^2 - v_L^2 (k_x^2 + k_L^2), \quad (4)$$

where v_L is a velocity approximately equal to the velocity of LA modes.

B. TO mode

$$\begin{aligned} u_x &= k_T (C e^{ik_T z} + D e^{-ik_T z}) e^{i(k_x x - \omega t)}, \\ u_z &= -k_x (C e^{ik_T z} - D e^{-ik_T z}) e^{i(k_x x - \omega t)}. \end{aligned} \quad (5)$$

These components satisfy the TO condition $\nabla \cdot \mathbf{u} = 0$. The electric fields associated with this mode are negligible. The dispersion relation is

$$\omega^2 = \omega_{TO}^2 - v_T^2 (k_x^2 + k_T^2), \quad (6)$$

where v_T is a velocity approximately equal to that of TA modes. Note that since $\omega_{TO} < \omega_{LO}$, in order for the frequency to be equal to a LO frequency k_T must be imaginary, corresponding to a TO interface mode (Fig. 1).

C. IP mode

$$\begin{aligned} u_x &= -ik_x (F e^{k_x z} + G e^{-k_x z}) e^{i(k_x x - \omega t)}, \\ u_z &= -k_x (F e^{k_x z} - G e^{-k_x z}) e^{i(k_x x - \omega t)}. \end{aligned} \quad (7)$$

These components satisfy the condition for transversely polarized waves $\nabla \cdot \mathbf{u} = 0$, and Eq. (7) is a valid approximation only in the unretarded limit (i.e., taking the speed of light to be infinitely large).¹⁵ The associated electric fields are¹⁶

$$E_x = -\rho_p u_x, \quad E_z = -\rho_p u_z, \quad \rho_p = \rho_0 \frac{\omega^2 - \omega_{TO}^2}{\omega_{LO}^2 - \omega_{TO}^2}. \quad (8)$$

Being a transverse electromagnetic wave, there is a vector potential \mathcal{A} given by

$$\mathbf{E} = -\frac{\partial \mathcal{A}}{\partial t}. \quad (9)$$

In the barriers, there are electric-field components whose amplitudes decay away from the interfaces. The dispersion relation for the IP mode and the barrier fields is just the usual one for electromagnetic waves:

$$\omega^2 = \frac{c^2 k^2}{\epsilon(\omega) \mu_0}, \quad (10)$$

where c is the velocity of light in vacuo and μ_0 is the per-

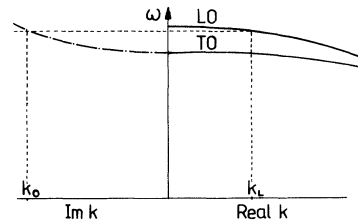


FIG. 1. Dispersion of bulk LO and TO modes.

meability of free space. The wave vector in this case is

$$k^2 = (k_x^2 + k_p^2), \quad (11)$$

where k_p is the z component, and $k_p \approx -ik_x$ in the unretarded limit. The frequency is determined by the boundary conditions. Conventionally these have been taken to be purely electromagnetic, which leads to the dispersion relation²

$$\omega^2 = \frac{\omega_{\text{LO}}^2 + r_0^{-1} \omega_{\text{TO}}^2 \pm e^{-k_x L} (\omega_{\text{LO}}^2 - r_0^{-1} \omega_{\text{TO}}^2)}{1 \pm r_0^{-1} \pm e^{-k_x L} (1 - r_0^{-1})}, \quad r_0 = \frac{\epsilon_\infty}{\epsilon_1}, \quad (12)$$

where L is the well width, ϵ_1 is the permittivity of the barrier, and ϵ_∞ is the high-frequency permittivity of the well. However, we assume nothing about the dispersion of IP modes other than that of Eq. (10).

D. Hybrids

All elastic and electromagnetic boundary conditions can be satisfied by a unique linear combination of LO, TO, and IP modes with common frequency and the common in-plane wave vector k_x ,

$$\mathbf{u} = \mathbf{u}_{\text{LO}} + \mathbf{u}_{\text{TO}} + \mathbf{u}_{\text{IP}}. \quad (13)$$

Hybrids of this type contain components which interact electrically with electrons in a simple band. (Note that the deformation-potential interaction will not be con-

sidered here.) The strongest interaction will be associated with long-wavelength LO and IP elements, the frequencies of which will lie nearer to ω_{LO} than to ω_{TO} . Restricting attention to this frequency range means taking the TO component to be an evanescent mode with $k_T = -ik_0$, where the following frequency condition is satisfied:

$$\begin{aligned} \omega^2 &= \omega_{\text{LO}}^2 - v_L^2 (k_x^2 + k_L^2) \\ &= \omega_{\text{TO}}^2 - v_T^2 (k_x^2 - k_0^2) = \frac{c^2}{\epsilon(\omega)\mu_0} (k_x^2 - k_p^2). \end{aligned} \quad (14)$$

The difference between k_x^2 and k_p^2 is small but finite, and can be neglected outside of Eq. (14). The wave vector k_0 is given by

$$k_0^2 = \frac{\omega_{\text{LO}}^2 - \omega_{\text{TO}}^2 - (v_L^2 - v_T^2) k_x^2 - v_L^2 k_L^2}{v_T^2}. \quad (15)$$

Those modes which interact most strongly with electrons have frequencies equal to or near the LO branch. For these modes k_0 is a bigger wave vector than any other and the approximation

$$\tanh k_0 L \approx 1, \quad (16)$$

where L is the well width, is valid. In what follows this approximation is assumed to hold.

The following two mode patterns emerge from a lengthy analysis. The first is (suppressing the time dependence)

$$u_x = 2ik_x A e^{ik_x x} \left[\sin k_L z - \{1 - p_1 \tanh(k_x L / 2)\} \sin(k_L L / 2) \frac{\sinh k_0 z}{\sinh(k_0 L / 2)} - p_1 \sin(k_L L / 2) \frac{\sinh k_x z}{\cosh(k_x L / 2)} \right], \quad (17a)$$

$$u_z = 2k_L A e^{ik_x x} \left[\cos k_L z - \frac{k_x^2}{k_L k_0} \{1 - p_1 \tanh(k_x L / 2)\} \sin(k_L L / 2) \frac{\cosh k_0 z}{\sin(k_0 L / 2)} - \frac{k_x}{k_L} p_1 \sin(k_L L / 2) \frac{\cosh k_x z}{\cosh(k_x L / 2)} \right] \quad (17b)$$

for $-L/2 \leq z \leq L/2$. The parameter p_1 is given by

$$p_1 = \frac{1}{s[\tanh(k_x L / 2) + r]}, \quad (18)$$

and the hybrid satisfies the condition

$$\cot(k_L L / 2) = \frac{k_x}{k_L} \left[p_1 + \frac{k_x}{k_0} [1 - p_1 \tanh(k_x L / 2)] \right]. \quad (19)$$

The pattern of the second type is

$$u_x = 2k_x A e^{ik_x x} \left[\cos k_L z - \{1 - p_2 \coth(k_x L / 2)\} \cos(k_L L / 2) \frac{\cosh k_0 z}{\sinh(k_0 L / 2)} - p_2 \cos(k_L L / 2) \frac{\cosh k_x z}{\sinh(k_x L / 2)} \right], \quad (20a)$$

$$u_z = 2ik_L A e^{ik_x x} \left[\sin k_L z + \frac{k_x^2}{k_L k_0} \{1 - p_2 \coth(k_x L/2)\} \cos(k_L L/2) \frac{\sinh k_0 z}{\sinh(k_0 L/2)} + \frac{k_x}{k_L} p_2 \cos(k_L L/2) \frac{\sinh k_x z}{\sinh(k_x L/2)} \right] \quad (20b)$$

for $-L/2 \leq z \leq L/2$ and

$$p_2 = \frac{1}{s[\coth(k_x L/2) + r]} \quad (21)$$

This hybrid satisfies the condition

$$\tan(k_L L/2) = -\frac{k_x}{k_L} \left[p_2 + \frac{k_x}{k_0} [1 - p_2 \coth(k_x L/2)] \right] \quad (22)$$

The ionic displacements for the four lowest-order modes in the limit $k_x L \rightarrow 0$ are shown in Fig. 2.

In the barriers there are no ionic displacements, only fields. These are given, for the first type, by

$$E_x = +iE_z = +2irs\rho_0 k_x A e^{ik_x x} e^{k_x [z+(L/2)]} p_1 \sin(k_L L/2), \quad z \leq -\frac{L}{2}, \quad (23a)$$

$$E_x = -iE_z = -2irs\rho_0 k_x A e^{ik_x x} e^{-k_x [z-(L/2)]} p_1 \sin k_L L/2, \quad z \geq \frac{L}{2}, \quad (23b)$$

and for the second type by

$$E_x = +iE_z = -2rs\rho_0 k_x A e^{ik_x x} e^{k_x [z+(L/2)]} p_2 \cos(k_L L/2), \quad z \leq -\frac{L}{2}, \quad (24a)$$

$$E_x = -iE_z = -2rs\rho_0 k_x A e^{ik_x x} e^{-k_x [z-(L/2)]} p_2 \cos(k_L L/2), \quad z \geq \frac{L}{2}. \quad (24b)$$

In these expressions ρ_0 is the charge density defined in Eq. (2), s is the ratio of fields in the IP and LO components, viz.,

$$s = \frac{\omega^2 - \omega_{TO}^2}{\omega_{LO}^2 - \omega_{TO}^2}, \quad (25)$$

and r is ratio of the IP permittivity in the well to that in the barrier, viz.,

$$r = \frac{\epsilon_\infty}{\epsilon_1} \frac{\omega^2 - \omega_{LO}^2}{\omega^2 - \omega_{TO}^2}. \quad (26)$$

In each hybrid there is a scalar potential ϕ associated with the LO component and a vector potential \mathcal{A} associated with the IP component. These are given below. For the first type,

$$\phi = 2\rho_0 A e^{ik_x x} \sin k_L z, \quad (27a)$$

$$\mathcal{A}_x = +\frac{2s\rho_0 k_x}{\omega} A e^{ik_x x} p_1 \sin(k_L L/2) \frac{\sinh k_x z}{\cosh(k_x L/2)}, \quad (27b)$$

$$\mathcal{A}_z = -\frac{2is\rho_0 k_x}{\omega} A e^{ik_x x} p_1 \sin(k_L L/2) \frac{\cosh k_x z}{\cosh(k_x L/2)}, \quad (27c)$$

and for the second type,

$$\phi = -2i\rho_0 A e^{ik_x x} \cos k_L z, \quad (28a)$$

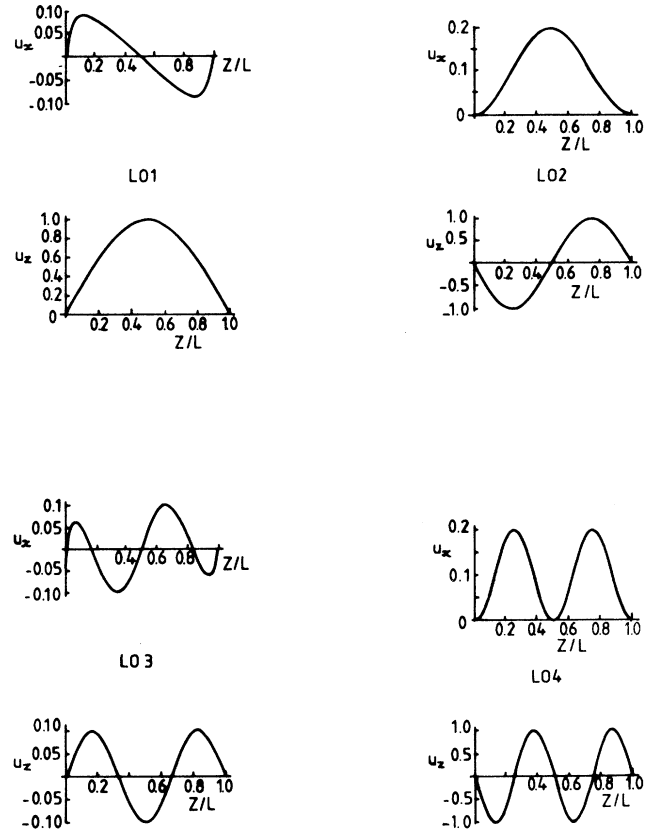


FIG. 2. Relative ion displacements for the four lowest modes in the limit $k_x L \rightarrow 0$ ($L = 38 \text{ \AA}$, GaAs).

$$\mathcal{A}_x = \frac{-2is\rho_0 k_x}{\omega} A e^{ik_x x} p_2 \cos(k_L L/2) \frac{\cosh k_x z}{\sinh(k_x L/2)}, \quad (28b)$$

$$\mathcal{A}_z = \frac{-2s\rho_0 k_x}{\omega} A e^{ik_x x} p_2 \cos(k_L L/2) \frac{\sinh k_x z}{\sinh(k_x L/2)}. \quad (28c)$$

It may be noted that the potentials are, in general, discontinuous at the interfaces. However, this discontinuity causes no problems regarding the interaction with an electron, as will be pointed out below. The discontinuity of the scalar potential was first pointed out in connection with the hydrodynamic (HD) model.

The normalization of the amplitude A is formally carried out via the techniques of quantum-field theory. Here, we adopt the informal approach of equating the energy of the hybrid with that of a simple harmonic oscillator. The energy of a particular mode, a mixture of mechanical and electromagnetic energies, is given by

$$U = \frac{1}{2} M \omega^2 \int_{-L/2}^{L/2} \mathbf{u}^* \cdot \mathbf{u} \frac{dz \sigma}{V_0} + \frac{1}{2} \varepsilon(\omega) \int_{-\infty}^{\infty} \mathbf{E}^* \cdot \mathbf{E} dz \sigma, \quad (29)$$

where σ is the surface area and M is the reduced mass. The limits on the integrals take into account that there is no mechanical energy in the barriers, but there is electromagnetic energy associated with the evanescent fields. Allowance has also been made for the equality of potential- and kinetic-energy components in a traveling wave.

Since $\varepsilon(\omega)=0$ for the LO component for all frequencies, only the IP component contributes electromagnetic energy. The ratio of electromagnetic to mechanical energy turns out to be small. In the well this ratio is

$$\frac{U_E}{U_M} = \frac{V_0 \varepsilon_p \rho_p^2}{M \omega^2} = \frac{(\omega^2 - \omega_{LO}^2)(\omega^2 - \omega_{TO}^2)}{\omega_{LO}^2(\omega_{LO}^2 - \omega_{TO}^2)}, \quad (30)$$

which has a maximum magnitude of $(\omega_{LO}^2 - \omega_{TO}^2)/4\omega_{LO}^2$, which is very small. Very little error will be incurred by neglecting the electromagnetic energy entirely, including that residing in the barrier. Retention of the electromagnetic energy poses no problems, but for simplicity we will define the coordinate χ of our equivalent oscillator solely in terms of mechanical energy. Thus

$$\chi^2 = \int_0^L \mathbf{u}^* \cdot \mathbf{u} \frac{dz \sigma}{V_0} \quad (31)$$

defines the amplitude A in terms of χ , which is then quantized in the usual way. The resultant quanta may be termed hybridons.

Carrying out this procedure leads to

$$A^2 = \frac{\chi^2}{2N\Delta^2}, \quad (32)$$

where, for the first type of solution,

$$\begin{aligned} \Delta^2 &= k_L^2 + k_x^2 + (k_L^2 - k_x^2) \frac{\sin k_L L}{k_L L} \\ &\quad - 4p_1 \frac{k_x}{L} \sin^2(k_L L/2) [2 - p_1 \tanh(k_x L/2)], \end{aligned} \quad k_L \text{ real}, \quad (33a)$$

$$\begin{aligned} \Delta^2 &= (\alpha_L^2 + k_x^2) \frac{\sinh \alpha_L L}{\alpha_L L} + \alpha_L^2 - k_x^2 \\ &\quad - 4p_1 \frac{k_x}{L} \sinh^2(\alpha_L L/2) [2 - p_1 \tanh(k_x L/2)], \end{aligned} \quad k_L = i\alpha_L, \quad (33b)$$

and for the second type of solution,

$$\begin{aligned} \Delta^2 &= k_L^2 + k_x^2 - (k_L^2 - k_x^2) \frac{\sin k_L L}{k_L L} \\ &\quad - 4p_2 \frac{k_x}{L} \cos^2(k_L L/2) [2 - p_2 \coth(k_x L/2)]. \end{aligned} \quad (34)$$

In Eq. (33b) the solution for k_L imaginary is noted for an interface mode which has been thought to exist (but which we show does not). Equations (33) and (34) have been derived for simplicity with neglect of the contribution by the TO component, which is very small if, as we have assumed, k_0 [Eq. (15)] is large.

E. Electron-hybridon interaction

The interaction energy involving an electron is

$$H = -e\phi + \frac{e}{m} \mathcal{A} \cdot \mathbf{p}, \quad (35)$$

where \mathbf{p} is the momentum operator and m is the free-electron mass. The electron-hybridon interaction is part Fröhlich-like, part electromagnetic. In the case of holes, or electrons in noncentral valleys, it would be necessary to include deformation-potential interactions involving all three components, in general. This would be essential in order to describe Raman scattering, for example.

In the barrier there is only the $\mathcal{A} \cdot \mathbf{p}$ interaction. Nevertheless continuity of interaction energy is guaranteed for an electron at rest with respect to the hybrid, since the operator \mathbf{p} can be replaced by $m\mathbf{v}$ where \mathbf{v} is the group velocity of the electron. Thus, if \mathcal{A} is the vector potential in the barrier, continuity of E_x and $\varepsilon(\omega)E_z$ implies that

$$\begin{aligned} \omega \mathcal{A}_{1x} &= -k_x \phi + \omega \mathcal{A}_x, \\ \mathcal{A}_{1z} &= r \mathcal{A}_z. \end{aligned} \quad (36)$$

The interaction in the barrier is $e(\mathcal{A}_{1x} v_x + \mathcal{A}_{1z} v_z)$ and in the well $e(-\phi + \mathcal{A}_x v_x + \mathcal{A}_z v_z)$, which are equal when $v_x = \omega/k_x$ and $v_z = 0$. Although neither scalar nor vector potential is continuous across the interface, the coherent interaction with an electron is continuous. In other treatments of the interaction, notably those using mode patterns derived from microscopic theory, there is no distinction made between scalar and vector potentials, all

potentials being regarded as scalar. However, the macroscopic theory developed here shows that the true situation is more subtle.

III. DISPERSION

To begin with, a word about nomenclature will be useful. For reasons which will become clear, solutions of the first type will be referred to as odd modes, solutions of the second type as even modes.

Both types of mode are triple hybrids of LO, TO, and IP waves satisfying mechanical and electromagnetic boundary conditions at each interface. Hybridization of LO and IP waves without TO involvement would be sufficient were there no dispersion. If for all modes $\omega = \omega_{LO}$, the parameters describing the effects of dispersion, s and r , would be, respectively, unity and zero. Cancellation of displacement in a LO/IP hybrid would then automatically cancel electric field and both boundary conditions would be satisfied. But in general $\omega \neq \omega_{LO}$, and the presence of a TO component is thereby required.

The properties of triple hybrids can best be discussed by focusing on the effect of varying the in-plane wave vector k_x . Because we neglect all effects associated with retardation, we cannot consistently begin with $k_x = 0$. Once k_x is finite, $s < 1$ and $r < 0$, and the mode patterns depend upon the relative sizes of $\tanh(k_x L / 2)$ and r and $\coth(k_x L / 2)$ and r . Note that $0 < s < 1$ and $-\infty < r < 0$ as ω approaches ω_{TO} or ω_{LO} . We consider various cases, first of all assuming $k_x L \ll 1$. Only in narrow wells can this condition coexist with that prohibiting k_x to be close to the light line.

$$\begin{aligned} \text{A. } (k_x L / 2) \ll |r| \text{ for odd modes;} \\ |r(k_x L / 2)| \ll 1 \text{ for even modes} \end{aligned}$$

For odd modes $p_1 \approx (rs)^{-1}$,

$$\cot(k_L L / 2) \approx \frac{k_x}{k_L rs}, \quad (37)$$

where $k_L L \approx n\pi$ with $n = 1, 3, 5$, etc. For even modes, $p_2 \approx s^{-1}$ and

$$\tan(k_L L / 2) \approx -\frac{k_x}{k_L s}, \quad (38)$$

where $k_L L \approx n\pi$ with $n = 2, 4, 6$, etc. These results explain the nomenclature. The pattern of the LO component and its scalar potential is that predicted by HD theory (Fig. 2). This regime has a range of validity which is very limited for low-order modes, but increases with decreasing well width. The condition written out explicitly is, with $k_x^2 \ll k_L^2$ and $\omega \approx \omega_{LO}$,

$$k_x L \ll \frac{2\epsilon_\infty v_L^2 k_L^2}{\epsilon_1(\omega_{LO}^2 - \omega_{TO}^2)}. \quad (39)$$

Note that in the case of the odd modes the barrier fields are substantial (p_1 is large) whereas in the case of the even modes they are insignificant (p_2 is very small). This property has evoked the nomenclature of ‘‘Coulomb

modes’’ and ‘‘mechanical modes’’ for the odd and even modes, respectively.⁹ In a superlattice, the long-range fields of the odd modes could induce phase changes in adjacent periods.

$$\begin{aligned} \text{B. } k_x L / 2 = -r \text{ for odd modes;} \\ r(k_x L / 2) = -1 \text{ for even modes} \end{aligned}$$

This is the condition for an upper-branch IP mode [in general $\tanh(k_x L / 2) + r = 0$]. For odd modes $p_1 \rightarrow \infty$ and hence $k_L L \rightarrow n\pi$ with $n = 2, 4, 6$, etc. In the expressions for the displacements, etc., the quantity $p_1 \sin(k_L L / 2)$ remains finite. Thus for this special case odd modes are forced into the parity of an IP mode. For even modes nothing changes very much (Fig. 3). The smallest value of k_x to satisfy this condition corresponds to the situation in which the LO1 wave vector k_L , and hence frequency, coincides with the LO2 mode. The general condition

$$\tanh(k_x L / 2) + r = 0 \quad (40)$$

traces a curve through the dispersion pattern of the hybrids, forcing odd modes to cross the even-modes dispersion.

There exists a corresponding effect associated with the lower IP branch when the general condition

$$\coth(k_x L / 2) + r = 0 \quad (41)$$

is satisfied, but this time it is the even-order modes which convert to odd order while the odd-order modes are unaffected.

$$\begin{aligned} \text{C. } k_x L / 2 \gg |r| \text{ for odd modes;} \\ |r|(k_x L / 2) \gg 1 \text{ for even modes} \end{aligned}$$

As k_x increases, the odd-order modes with frequencies coinciding with the upper-branch IP modes continue to increase in wave vector k_L , and eventually they settle near the wave vector of the next-highest-order odd modes (Fig. 3 depicts the mode patterns). In contradiction to that, the lower-branch IP modes force the even modes to reduce k_L and settle near k_L of the next-lowest-order even mode. Figure 4 depicts the dispersion diagram. All

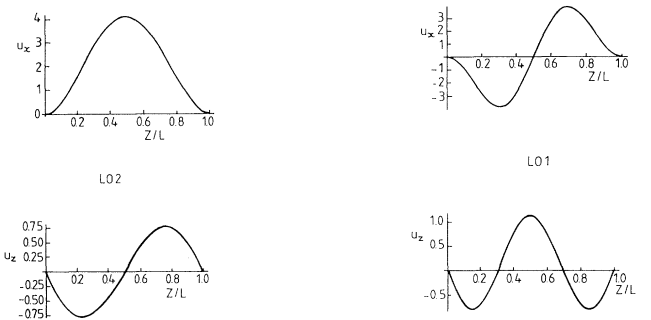


FIG. 3. Relative ion displacements for the LO2 and LO3 modes when $k_x L = 3$. The even-order mode shows no change, but the LO3 mode is now the shifted LO1 mode.

the modes are essentially guided LO hybrids, but they mimic the dispersion of IP modes near those limited regions of k_x where either of the conditions in Eqs. (40) and (41) is satisfied. There are no conventional IP modes at all, though it is clear that Raman-scattering experiments could easily give the impression that true IP modes existed. Note that in all of this IP-induced dispersion the number of modes remains constant (equal to N , the number of unit cells in the well minus two).

The shift of odd modes from n to near $n+2$, which occurs for narrow wells in the regime $k_x L \approx 1$, can be ap-

proximately quantified by putting $\tanh(k_x L/2) \approx (k_x L/2)$, $s=1$, and $r=0$ in Eq. (19), and therefore $\tan(k_L L/2) = (k_L L/2)$. This provides a rough estimate for k_L which is especially good for the $n=1-3$ transition, giving $k_L L \approx 2.8\pi$.

When $k_x L \ll 1$, as we have assumed, regimes III B and III C are applicable only to modes whose frequencies lie near ω_{LO} (odd modes) or ω_{TO} (even modes). [Note that in the case of even modes the frequency should not lie too near ω_{TO} , otherwise our assumption of Eq. (16) would not apply. However, the general behavior does not depend

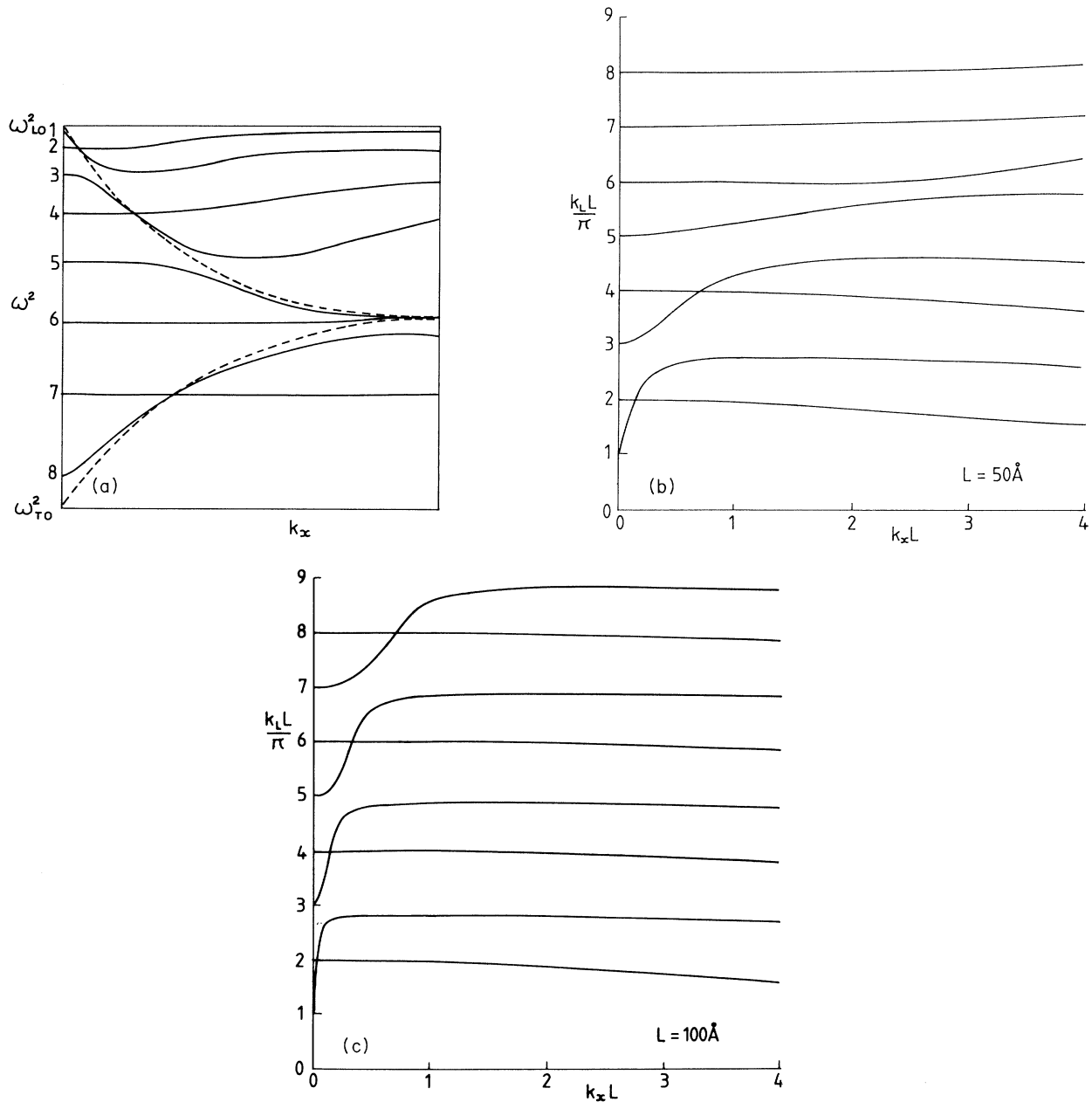


FIG. 4. Dispersion. (a) Schematic. The wave vector of the LO component in a GaAs quantum well as a function of the in-plane wave vector is plotted in (b) $L = 50 \text{ \AA}$, (c) $L = 100 \text{ \AA}$. These curves are solutions of Eqs. (19) and (22) for the first eight modes.

critically on this.] For $k_x L \geq 1$, Eqs. (40) and (41) already extend regime III B. As k_x increases, $\tanh k_x L / 2 \rightarrow 1$, and this reduces the dependence of the parameters p_1 and p_2 on k_x . As a result, the downward shift of frequency which the odd modes undergo as a consequence of IP-induced dispersion reverses, but the recovery is only toward the basic even-mode frequency, and the even-mode frequency moves upward toward the original odd-mode frequency. Corresponding processes occur in the lower portion of the dispersion diagram. In the limit, therefore, odd and even LO components exchange parities. Thus at low $k_x L$, the LO component is that given by HD theory, and at high $k_x L$ it is that given by DC theory.

Modes move around in frequency but they do not ever disappear. It is of interest to examine the possibility of there being an interface mode in addition to the hybrids described above, which are essentially guided modes (k_L discrete). Putting $\tanh(k_x L / 2) = 1$ in the dispersion equations suggests that the odd modes include an interface mode in which $k_L = -i\alpha_L$, and Eq. (19) becomes

$$\frac{\tanh(\alpha_L L / 2)}{(\alpha_L L / 2)} = \frac{s(1+r)}{(k_x L / 2)}, \quad (42)$$

from which it may be deduced that indeed an interface mode is allowed. However, it is important to retain the full dispersion expression, Eq. (19). When this is done the solution which emerges is, for all k_x ,

$$\alpha_L = k_x. \quad (43)$$

This condition corresponds to $\omega = \omega_{LO}$, i.e., $s = 1$ and $r = 0$. Equation (17) shows that this means that u_x and u_z are zero for all z , and this is consistent with Eq. (33b), which becomes $\Delta^2 = 0$, corresponding to zero energy. This interface mode is therefore a null mode, a con-

clusion that is consistent with there being no loss of guided modes with increasing k_x . Microscopical theory confines the maximum number of LO hybrids to N , the number of unit cells, and this complement is entirely filled by guided modes, including those with frequencies less than ω_{TO} (not treated here). However, the $n = 0$ mode, which usually manifests itself as an interface mode, is not allowed in the case of rigid boundaries.

IV. ELECTRON-HYBRIDON SCATTERING RATES

Model scattering rates can be obtained by assuming infinitely deep well envelope wave functions for the electron, i.e.,

$$\Psi = \left[\frac{2}{V} \right]^{1/2} e^{i\mathbf{k} \cdot \mathbf{r}} \times \begin{cases} \cos K_n z, & K_n L = n\pi, \quad n = 1, 3, \text{ etc.} \\ \sin K_n z, & K_n L = n\pi, \quad n = 2, 4, \text{ etc.} \end{cases} \quad (44)$$

In the effective-mass approximation, the matrix element quantifying the transition rate between state 1 and state 2 is

$$M = \int_{\mathbf{r}} \int_{-L/2}^{L/2} \psi_2^* \left[-e\phi - \frac{i\hbar e}{m^*} \left[\mathcal{A}_r \cdot \frac{\partial}{\partial \mathbf{r}} + \mathcal{A}_z \frac{\partial}{\partial z} \right] \right] \psi_1 dz d\mathbf{r} \quad (45)$$

$$= \delta_{\mathbf{k}} G, \quad (46)$$

where $\delta_{\mathbf{k}}$ symbolizes the conservation of crystal momentum in the plane, viz.,

$$K_{x1} + k_x = K_{x2}, \quad K_{y1} = K_{y2}, \quad (47)$$

and

$$G = \frac{2}{L} \int_{-L/2}^{L/2} \psi_2(z) \left[-e\phi\psi_1(z) - \frac{i\hbar e}{m^*} \left[(iK_{x1}\mathcal{A}_x + iK_{y1}\mathcal{A}_y)\psi_1(z) + \mathcal{A}_z \frac{\partial \psi_1(z)}{\partial z} \right] \right] dz. \quad (48)$$

The potentials are given in Eqs. (27) and (28).

For scattering within the lowest subband, the odd modes contribute nothing, whereas interaction with even modes leads at threshold to

$$G_{11}(k_L) = -2ie\rho_0 A \frac{2}{L} \left[\frac{4K_1^2 \sin(k_L L / 2)}{k_L(4K_1^2 - k_L^2)} - \frac{s\hbar}{m^* \omega} p_2 \frac{2K_1^2(K_{x1} + K_{x2}) \cos(k_L L / 2)}{(4K_1^2 + k_x^2)} \right]. \quad (49)$$

Here A is given by Eqs. (32) and (34), s by Eq. (25), and p_2 by Eq. (21). The wave vector k_L obeys the dispersion relation of Eq. (22). For the case of narrow wells ($k_x L < 1$), $k_L L \approx 2n\pi$, and this makes the first term in the brackets essentially zero unless $k_L L = 2\pi$, i.e., only in the LO2 hybrid does the LO component contribute to intrasubband scattering in the lowest subband. This was also the prediction of HD theory.¹⁷ In this limit ($k_x L / 2$)coth($k_x L / 2$) ≈ 1 and $\cos(k_L L / 2) \approx -1$, and thus

$$G_{11} \approx -2ie\rho_0 A \left[\frac{1}{2} + \frac{4}{4 + (k_x^2 L^2 / \pi^2)} \right]. \quad (50)$$

Application of the Fermi golden rule¹⁷ then leads to the rate for an electron with energy $\hbar\omega$:

$$W \approx \frac{1}{2} W_0 \left[\frac{\hbar\omega}{E_1} \right]^{1/2} \frac{1}{4 - (\hbar\omega/E_1)} \left[1 + \frac{8}{4 + (\hbar\omega/E_1)} \right]^2 \quad (51a)$$

$$\approx \frac{1}{2} W_0 \left[\frac{\hbar\omega}{E_1} \right]^{1/2} \frac{9}{4} [1 - (\hbar\omega/12E_1)], \quad (51b)$$

where

$$W_0 = \frac{e^2}{4\pi\hbar} \left[\frac{2m^*\omega}{\hbar} \right]^{1/2} \left[\frac{1}{\epsilon_\infty} - \frac{1}{\epsilon_s} \right] \quad (52)$$

and E_1 is the subband energy $\hbar^2\pi^2/2m^*L^2$ (Fig. 5). Apart from the sign in the denominator of Eq. (51), this rate in the limit $L \rightarrow 0$ is the HD rate increased by a factor 9 which is exactly the rate produced by Huang-Zhu guided modes. We may note that under the special circumstances considered here the distinction between vector and scalar potentials turns out to be irrelevant in determining the rate. The negative sign in the denominator of Eq. (51a) arises from the normalizing factor Δ^2 , which in this limit ($k_x^2 \ll k_L^2$) is $\Delta^2 \approx k_L^2 - k_x^2$. This relation reflects the reduction in mechanical energy due to the interfering effect of the LO and IP modes.

The total rate is given by summing the contributions derived from the IP components of other even modes. The magnitudes of these contributions reduce with increasing mode number n , being proportional to n^{-2} in this regime. Summing converts Eq. (51b) in the limit $\hbar\omega/E_1 \ll 1$ to

$$W = \frac{1}{2} W_0 \left[\frac{\hbar\omega}{E_1} \right]^{1/2} \left[\frac{5}{4} + \frac{\pi^2}{6} \right], \quad (53)$$

which amounts to an increase of some 30%.

For wide wells such that $k_x L > 1$, dispersion drives the LO2 mode to the old LO1 frequency, i.e., $k_L L \approx \pi$. In this limit, $s \approx 1$, $r \approx 0$, $p_2 \approx 1$, and $\cos(k_L L/2) \approx -k_L/k_x$,

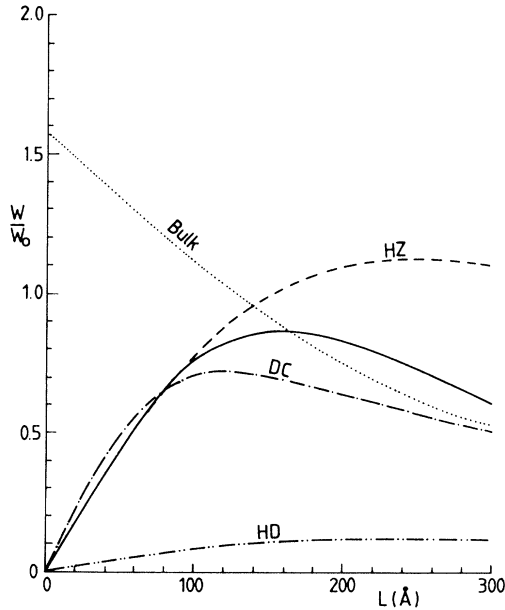


FIG. 5. Intrasubband scattering rate (continuous curve) associated with the LO2 mode. Also shown are the rates predicted by the bulk, DC, HD, and HZ guided-mode models. All rates refer to emission by an electron in the lowest subband with energy $\hbar\omega$.

and therefore, since the LO component in all “even” modes can now participate,

$$G_{11j} \approx -2ie\rho_0 A \frac{8}{\pi} \frac{1}{(2j-1)[4-(2j-1)^2]}, \quad j=1,3, \text{ etc.} \quad (54)$$

giving for the leading term ($j=1$),

$$W = \frac{1}{2} W_0 \left[\frac{\hbar\omega}{E_1} \right]^{1/2} \left[\frac{16}{3\pi} \right]^2 \frac{1}{1+(\hbar\omega/E_1)}. \quad (55)$$

This is the rate that is given by DC theory,¹¹ which is, incidentally, close to the rate obtained using a bulk-phonon spectrum and the momentum-conservation approximation^{18,19} in this regime of well width where $(\hbar\omega/E_1) \gg 1$; viz.,

$$W = \frac{1}{2} W_0 \left[\frac{\hbar\omega}{E_1} \right]^{1/2} \left[2 \left[\frac{E_1}{\hbar\omega} + \frac{1}{4+(\hbar\omega/E_1)} \right] \right]. \quad (56)$$

Thus our hybrid solution encompasses the results of both of the single-mode theories. For $k_x L \ll 1$ it reproduces the symmetry of the HD result and for $k_x L \gg 1$ it reproduces the DC result. This property is in line with the notion that purely mechanical boundary conditions can be approximately valid only when the tangential displacement, and hence tangential field, is small, and purely electromagnetic boundary conditions can be approximately valid only when the normal displacement is small.

It must be emphasized that Eq. (49) for the matrix element exhausts the scattering potential of LO and IP modes. The modes with which the electron interacts are all guided in the sense that the wave vector of the LO component is always constrained. Hybridization forces this guided property on both TO and IP interface components, with the consequence that the scattering strength via the electric and magnetic interactions diminishes as well as becomes narrow. It also precludes additional scattering from IP modes since, in pure form, they do not exist. Calculations which take the scattering of IP modes to be additional to that of HZ modes appear, therefore, to include the effects of IP scattering twice over, and they consequently lead to an overestimate of the scattering rate.

Turning to the intersubband rate between subbands 2 and 1, we note first that for an electron at the bottom of subband 2 emitting a hybridon, conservation of energy entails that

$$\frac{\hbar^2 k_x^2}{2m^*} = \frac{3\hbar^2 \pi^2}{2m^* L^2} - \hbar\omega. \quad (57)$$

For the transition to be possible, $L \leq (2m^*\omega/3\pi^2\hbar)^{1/2}$ (about 217 Å in GaAs). When L is at its maximum, $k_x=0$, but for narrow wells k_x will not be small. In many cases of interest, therefore, the LO1 hybrid will have converted to LO3. This is important since even modes do not contribute to scattering between adjacent subbands. For odd modes in general,

$$G_{21} = 2e\rho_0 A \sum_{k_L} \frac{2}{L} \left[\frac{4k_L K_1 K_2 \cos(k_L L / 2)}{[(K_2 + K_1)^2 - k_L^2][(K_2 - K_1)^2 - k_L^2]} + \frac{s\hbar k_x p_1}{m^* \omega} \frac{2K_1 K_2 [(K_{x1} + K_{x2})k_x - K_2^2 + K_1^2] \sin(k_L L / 2)}{[(K_2 + K_1)^2 + k_x^2][(K_2 - K_1)^2 + k_x^2]} \right]. \quad (58)$$

In the situation under consideration $K_1 = \pi/L$, $K_2 = 2\pi/L$, $K_{x1} = k_x$, $K_{x2} = 0$, $p_1 \approx s^{-1}$. An approximate analytic expression can be obtained by assuming $k_L L \approx 3\pi$ and $\cos(k_L L / 2) \approx 0$. [More accurately, we should solve Eq. (19) for k_L .]

We obtain

$$G_{21} = 2e\rho_0 A \left[\frac{1}{2} + g_1 \right], \quad (59a)$$

$$g_1 = \frac{16}{\pi} \frac{[3 - (\hbar\omega/E_1)]^{1/2}}{[12 - (\hbar\omega/E_1)][4 - (\hbar\omega/E_1)]}. \quad (59b)$$

In the same regime the normalization factor becomes

$$\Delta^2 = k_L^2 + k_x^2(1 - g_2), \quad (60a)$$

$$g_2 = \frac{4}{\pi[3 - (\hbar\omega/E_1)]^{1/2}}. \quad (60b)$$

The intersubband scattering rate contributed by the converted LO1 hybrid is then (Fig. 6)

$$W = \frac{1}{2} W_0 \left[\frac{\hbar\omega}{E_1} \right]^{1/2} \frac{(1 + 2g_1)^2}{9 + (1 - g_2)[3 - (\hbar\omega/E_1)]}. \quad (61)$$

In the limit of narrow wells $g_1 \rightarrow (\pi\sqrt{3})^{-1}$ and $g_2 \rightarrow 4g_1$.

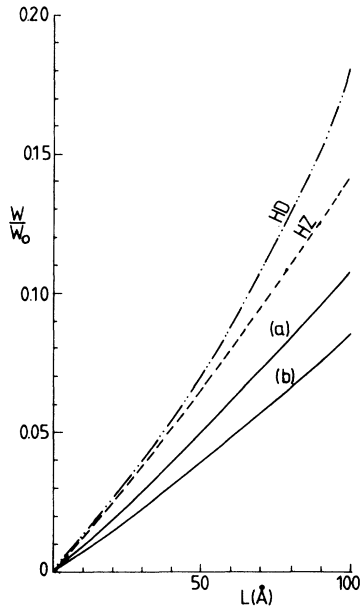


FIG. 6. Intersubband scattering rate for lowest-order mode [continuous curves: (a) $k_L L = 2.8\pi$, (b) $k_L L = 3\pi$]. Also shown are the total rates predicted by the HD and HZ models. (The rate for the DC model is close to the HZ rate.) All rates refer to emission by an electron at the bottom of subband 2. The total rate in the present theory is about 30% above curve (a).

With g_1 and g_2 zero the rate is just that of HD theory¹⁷ for the LO3 component. The factors g_1 and g_2 derive from interference effects of the IP component. Equation (61) becomes increasingly inaccurate as the well width approaches the resonant condition [$3 - (\hbar\omega/E_1) = 0$], and recourse must then be made to the general expression of Eq. (58) and to the details of dispersion of the LO1 hybrid. Figure 6 also shows the rate obtained using the more accurate relation $k_L L = 2.8\pi$. To obtain the total rate means summing the contributions of all the odd modes. As in the case of intrasubband scattering, this is expected to increase the LO1 rate by about 30%, and bring it close to the HZ rate.

V. DISCUSSION

Perhaps the most striking conclusion that hybridon continuum theory arrives at is that pure IP modes do not exist in realistic systems. At first this seems to be at variance with many observations of Raman scattering.²⁰⁻²² Some of these have been from relatively thick slabs ($L > 1000 \text{ \AA}$), in which the combination of high density of modes per unit frequency interval and IP-induced dispersion would make it difficult to distinguish the prediction of conventional IP theory from that of the theory presented here. Only in thin wells could such a distinction be possible, and even so to distinguish between pure IP dispersion and the IP-induced dispersion of hybrids will need careful measurement. Nevertheless, hybrid theory suggests that IP modes as conventionally described simply do not exist. Their power to interact with electrons is, however, incorporated in each hybrid, but it is heavily modified by energy normalization, often dominated by the mechanical energy of the LO components to which they are coupled. As a result of the lack of all interface modes in this system, the guided nature of the hybrids ensures the weakening of the Fröhlich and magnetic interactions as wells narrow. Only in cases where the dispersion of LO modes is insufficient to allow hybridization over the wide range of frequencies will this conclusion need modification.

Besides linking the DC and HD theories in a synthesis, hybrid theory has been forced to elucidate the question of continuity of potential which HD theory has consistently denied as being necessary, but which is still commonly assumed. It turns out that neither scalar potential nor vector potential is in general continuous across an interface, but continuity is reserved for the energy of coherent interaction with an electron.

Triple hybridization is generally required for all polar slabs whatever the mechanical boundary conditions, though in some special circumstances double hybrids can suffice. In nonpolar slabs, IP modes do not occur and LO

modes do not possess long-range fields, so double hybrids of LO/TO are adequate to satisfy mechanical boundary conditions. In general the latter must ensure continuity of energy flow and of the relevant stress components.

Hybrid theory appears to be remarkably successful in describing the envelopes of the vibrations predicted by microscopic theory, in spite of involving large wave vectors such as k_0 [see Eq. (15)], and of course as a continuum theory it is more useful for describing electron scattering. Nevertheless, real materials are elastically anisotropic and atomic, and these properties have been ignored. Akero and Ando²³ have pointed out that mechanical boundary conditions on relative ionic displacement do not accurately reflect the true situation at an interface, though they may be a reasonable approximation provided the differences between force constants and mass ratios are small. In this respect the situation is analogous to that for electrons, where if envelope functions are to be matched the difference between effective masses must be small. Reservations of this kind have to be borne in mind, but like effective-mass theory, it is expected that hybrid theory will find wide application.

Finally, it is important to point out that not all systems allow hybridization of the kind discussed here to occur over the frequency range between ω_{TO} and ω_{LO} . In AlAs, for example, LO dispersion is too weak to allow guided LO modes to hybridize with IP modes except over the narrow range of LO frequencies. Nevertheless IP modes must still satisfy mechanical boundary conditions, and in order to do this it is necessary for them to hybridize with an LO evanescent mode belonging to the complex band structure connecting LO and LA (longitudinal-acoustic) branches, as well as with a TO evanescent mode. Such hybridization can be described by the theory presented

here with the substitution $k_L \rightarrow \kappa_\Lambda + id$, with k_L at or close to the zone boundary. Effectively, this allows IP modes to retain their familiar mode patterns except very near the interfaces in the frequency range between ω_L at the zone boundary and ω_{TO} . This weak hybridization of some IP modes in AlAs will strengthen the interaction with electrons in the AlAs/GaAs system as wells narrow. However, AlAs is unusual in this respect; in many other III-V systems the IP modes will suffer strong hybridization with LO-guided modes, as discussed in this paper. However, the more polar the material the more AlAs-type behavior will occur.

Note added in proof. Since this paper was submitted, there have been two developments which are worth a brief mention since they provide some deepening of the understanding of optical-mode hybridization. One is that in ionic slabs with stress-free surfaces the LO, TO, and IP modes are only very weakly hybridized, which means that Fuchs-Kliwer modes remain a good approximation; the other is that provided that only the scattering rate is required it can now be shown that the vector potential of the IP mode can be satisfactorily replaced by a scalarlike potential in the unretarded limit (as is usually assumed without proof). We hope to report on these issues shortly.

ACKNOWLEDGMENTS

The author would like to express his appreciation for many discussions with Dr. M. Babiker and Dr. N. Constantinou, which have been extremely useful. He is also grateful to S.E.R.C., the U.S. Office of Naval Research, and the U.S. Army Research Office for supporting this work.

¹B. K. Ridley and M. Babiker, Phys. Rev. B **43**, 9096 (1991).

²R. Fuchs and K. L. Kliewer, Phys. Rev. **140**, A2076 (1965).

³M. Babiker, J. Phys. C **19**, 683 (1986).

⁴K. Huang and B.-F. Zhu, Phys. Rev. B **38**, 2183 (1988).

⁵B.-F. Zhu, Phys. Rev. B **38**, 7694 (1988).

⁶K. Huang and B.-F. Zhu, Phys. Rev. B **38**, 13 377 (1988).

⁷F. Bechstedt and H. Gerecke, Phys. Status Solidi B **154**, 565 (1989).

⁸F. Bechstedt and H. Gerecke, Phys. Status Solidi B **156**, 157 (1989).

⁹H. Gerecke and F. Bechstedt, Phys. Rev. B **34**, 7053 (1991).

¹⁰A. Fasolino, E. Molinari, and K. Kunc, Phys. Rev. B **41**, 8302 (1990).

¹¹S. Rudin and T. L. Reinecke, Phys. Rev. B **41**, 7713 (1990); **43**, 9288 (1991).

¹²R. Haupt and L. Wendler, Phys. Rev. B **44**, 1850 (1991).

¹³H. Rucker, E. Molinari, and P. Lugli, Phys. Rev. B **44**, 3463 (1991).

¹⁴B. K. Ridley, Phys. Rev. B **44**, 9002 (1991).

¹⁵K. L. Kliewer and R. Fuchs, Phys. Rev. **144**, 495 (1966).

¹⁶B. K. Ridley, *Quantum Processes in Semiconductors* (Oxford University Press, Oxford, 1988).

¹⁷B. K. Ridley, Phys. Rev. B **39**, 5282 (1989).

¹⁸B. K. Ridley, J. Phys. C **15**, 5899 (1982).

¹⁹F. A. Riddoch and B. K. Ridley, J. Phys. C **16**, 6971 (1983).

²⁰R. E. Camley and D. L. Mills, Phys. Rev. B **29**, 1695 (1984).

²¹A. K. Sood, J. Menendez, M. Cardona, and K. Ploog, Phys. Rev. Lett. **54**, 2115 (1985).

²²M. Nakayama, M. Ishida, and N. Sano, Surf. Sci. **228**, 131 (1990).

²³H. Akero and T. Ando, Phys. Rev. B **40**, 2914 (1989).